Superlattices and Microstructures, Vol. 23, No. 1, 1998

Polarization-dependent intersubband absorption and normal-incidence infrared detection in p-type Si/SiGe quantum wells

P. KRUCK, A. WEICHSELBAUM, M. HELM, T. FROMHERZ, G. BAUER
Institut für Halbleiterphysik, Universität Linz, A-4040 Linz, Austria

J. F. NÜTZEL, G. ABSTREITER
Walter Schottky Institut, TU München, D-85784 Garching, Germany

(Received 15 July 1996)

A detailed study of the polarization dependence of subband absorption and photoconductivity in pseudomorphic p-type $Si/Si_{0.64}Ge_{0.36}$ quantum wells is presented. The fabricated quantum well infrared photodetectors (QWIP) show a photoresponse between 3 and 8 μm with a peak-wavelength of $\lambda_p = 5\ \mu$m under normal incidence illumination. At the optimum bias operating point a detectivity $D^*_\lambda = 2 \times 10^{10}$ cm $\sqrt{\text{Hz}}$ W^{-1} is achieved. On the basis of a self-consistent six-band Luttinger–Kohn calculation the p- and s-polarized intersubband transitions, leading to the observed photoconductivity, are identified.

Key words: Si/SiGe, intersubband absorption, infrared detector.

Optical transitions between confined subbands in doped quantum wells have attracted much interest because they allow the realization of sensitive infrared detectors for the spectral range between 3 and 20 μm [1, 2]. The high quantum efficiency and uniformity of the so-called quantum well infrared photodetectors (QWIP) makes them especially attractive for thermal imaging applications. Up to now most of the work has been concentrated on n-doped GaAs QWIPs where the superior transport of the photoexcited electrons above the barriers results in detectivities as high as $D^*_\lambda \geq 10^{11}$ cm $\sqrt{\text{Hz}}$ W^{-1}. For this purpose optical couplers like gratings [3] or random scatterers [1] have been employed, which provide a component of the electric field parallel to the growth direction necessary for intersubband absorption in n-doped quantum wells due to the symmetry of the conduction band at the Γ-point.

In p-doped QW the restriction introduced by the quantum mechanical selection rule is removed due to the coupling of heavy-hole, light-hole and spin–orbit split-off subbands [4–7]. The desirable normal-incidence detection without optical couplers has been demonstrated in p-type GaAs [8] as well as p-type SiGe QWIPs [4, 6]. A Si-based QWIP offers the additional advantage of having the same thermal expansion coefficient as the Si readout electronics, an aspect which is essential for the realization of large detector arrays operating under low temperature conditions ($T \approx 80$ K). Also a direct monolithic integration with MOS readout circuitry is possible [9]. Another promising detector concept with considerable quantum efficiencies, which should be mentioned in this context, is the single heterojunction SiGe/Si device, where the free-carrier absorption

0747–7171/98/010061 + 06 $25.00/0 sm960308

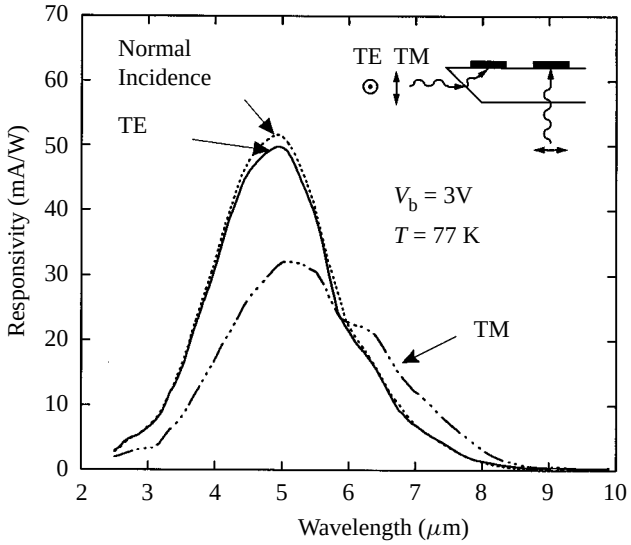

Fig. 1. Photoresponse spectra measured in TE (full line) und TM (dashes–dots) polarization for a bias voltage of $V_b = 3$ V and temperature $T = 77$ K. The normal-incidence spectrum recorded under the same operating conditions is plotted for comparison (dashed line). The illumination geometries are shown in the inset.

followed by internal photoemission over the heterojunction barrier is used for IR detection [9, 10]. In this letter we report the results of our experimental and theoretical work on a bound-to-continuum $Si_{0.64}Ge_{0.36}$/Si QWIP operating between 3 and 8 μm. The investigations were restricted to moderately doped structures where free-carrier and many-body effects do not complicate the understanding of the relation between intersubband absorption and photoconductivity [5, 7].

The detector samples investigated in this work were grown on a (001) Si substrate ($\rho \sim 1500\ \Omega$ cm) by molecular beam epitaxy. The structure consists of 10 periods of $L_w = 2.5$ nm quantum wells (boron-doped $p = 4 \times 10^{18}$ cm^{-3}) separated by undoped $L_B = 50$ nm Si barriers, and enclosed between two contact layers ($p = 4 \times 10^{18}$ cm^{-3}), where the top and bottom layer are 100 nm and 300 nm thick, respectively. To perform dark-current and photoconductivity measurements the samples were processed into 200 μm $\times$ 200 μm square mesas by reactive ion etching (RIE) in a CF_4 plasma, followed by a standard Al metallization for contacting.

The measurement of the normal-incidence responsivity, which is decisive for array applications, was performed with the backside of the Si wafer polished to allow illumination through the substrate. Since we are also interested in the polarization dependence of the photoconductivity, another sample was prepared in waveguide geometry. Here the transverse magnetic (TM or p-polarized) and transverse electric (TE or s-polarized) polarized light is coupled into the mesa via a wedged 38° facet, resulting in a 52° illumination of the active layers. During the photoresponse measurements the spectrally dispersed radiation of a calibrated blackbody source enters the liquid-helium flow cryostate through a ZnSe window. The resulting responsivity spectra taken at $T = 77$ K for a bias voltage of $V_b = 3$ V for TE and TM polarization is plotted in Fig. 1. A peak responsivity of 50 mA W^{-1} is obtained which increases to 76 mA W^{-1} at $V_b = 4$ V (not shown). For the discussion of the spectra note that the TM mode contains z (z is the growth direction) as well as the xy polarized components of the electromagnetic field. In strong contrast to n-type QWIPs the shape of the TE and TM spectrum is mainly determined by the photoresponse to in-plane polarized radiation. A slight modification of the TM spectrum with respect to the TE spectrum is observed in the cutoff region around 7 μm. We measure a long-wavelength cutoff $\lambda_c = 7.8$ μm and $\lambda_c = 6.9$ μm for TM and TE, respectively.

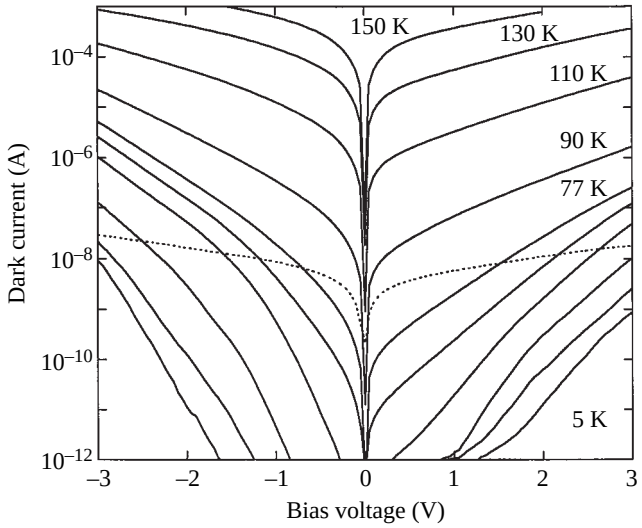

Fig. 2. Dark Current I_d versus bias voltage V_b (full line) for the Si/SiGe QWIP measured for temperatures $T = 5$, 10, 30, 60, 70, 77, 90, 110, 130, and 150 K. The photocurrent I_p generated by the room temperature background radiation for a field-of-view $fov = 180^\circ$ is plotted as dashed line. I_p is obtained by subtraction of two current–voltage curves measured with and without cold shield at $T = 77$ K. Positive bias means mesa top positive.

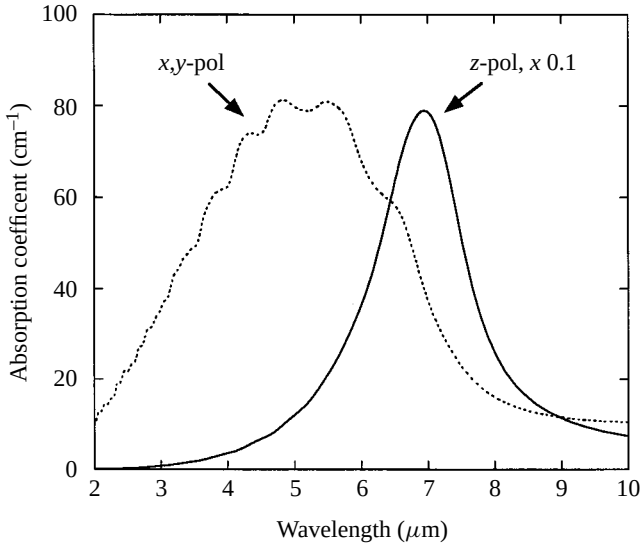

Fig. 3. Absorption spectrum calculated for the present QWIP structure. The broken line shows the absorption for light polarized in xy direction, the full line shows the absorption spectrum for z polarization. The absorption coefficient is normalized to the multiquantum well period. The z-polarized absorption coefficient has been multiplied by 0.1.

The peak position at $\lambda_p = 5\ \mu$m is nearly identical for both polarizations. The normal incidence responsivity spectrum measured under the same operating conditions coincides with the waveguide TE spectrum (cf. Fig. 1).

A further discussion of the detector performance has to focus on the dark current and the detectivity. Dark-current bias curves were measured as a function of temperature between 5 and 150 K (Fig. 2). For bias voltages smaller than $V_b = 1$ V and temperatures lower than $T = 30$ K the dark current is so small ($I_d < 10^{-12}$ A) that it could not be measured. Between $T = 70$ and $T = 150$ K, that is over more than five orders of magnitude, the dark current is consistent with thermionic emission [1] with an activation energy of $\Delta E = 143$ meV (at $V_b = 2$ V), consistent with the long-wavelength cut-off for the z-polarization. Due to the thick barriers, tunneling is of minor importance for temperatures down to 30 K.

The detectivity, $D^*_\lambda = R_p\sqrt{A}/i_n$, can be determined by evaluating the shot noise expression $i_n = \sqrt{4eI_d g\Delta f}$ (where A is the detector area, Δf is the measurement bandwidth and g is the gain). For the present device the gain is estimated to be $g = 0.3$ [6]. Together with the dark current $I_d = 1.4 \times 10^{-6}$ A at $V_b = 4$ V we obtain $D^*_\lambda = 3 \times 10^9$ cm $\sqrt{\text{Hz}}\,\text{W}^{-1}$. A distinct increase of the detectivity is achieved by reducing the bias voltage to $V_b = 0.8$ V, since the dark current drops more rapidly with decreasing bias voltage than does the responsivity. At the optimum bias point, where the dark current is as low as $I_d = 1.1 \times 10^{-9}$ A ($T = 77$ K), the detectivity reaches up to $D^*_\lambda = 2 \times 10^{10}$ cm $\sqrt{\text{Hz}}\,\text{W}^{-1}$. Therefore the detectivity of our SiGe/Si QWIP is comparable to the p-type GaAs/AlGaAs QWIP reported in [8]. Another important figure of merit, the background limited infrared performance (BLIP), was measured by allowing the room-temperature blackbody radiation to enter the cryostat through the ZnSe window and illuminate the detector under normal incidence. The background photocurrent I_p generated by a full-cone field-of-view (180°) is plotted as a broken line in Fig. 2. For a bias voltage $V_b = 0.8$ V BLIP is achieved at $T = 85$ K.

A self-consistent six-band Luttinger–Kohn calculation including the in-plane dispersion [5, 11, 12] was performed to understand the origin and spectral position of the observed photoconductivity†. The calculated absorption spectrum for xy and z polarized radiation is plotted in Fig. 3. The z-polarized peak can be identified with the HH1–HH2 transition and is an order of magnitude larger than the xy-polarized absorption (not in accordance with the photoresponse spectra—see below) . For the present well dimensions the HH2-like final state is only weakly bound, resulting in the formation of a miniband in the k_z-direction. As a consequence the absorption line is rather broad and asymmetric. The situation is more complicated for the xy absorption spectrum, since several bound-to-continuum transitions at $k_\parallel = 0$ and at finite in-plane wavevectors contribute. However, the involved transitions can be identified by means of a contour plot of the oscillator strength as a function of the final state and the in-plane wavevectors up to the Fermi wavevector, $k_F = 0.03$ Å^{-1} (Fig. 4). Excited states with significant oscillator strength to the ground state are labeled by a triplet of numbers to characterize the contributions of the HH, LH and SO valence band. From the plot of the in-plane dispersion (Fig. 4) the corresponding energy difference between the ground state and the excited state can be determined. The results of the bandstructure calculation together with the subsequent evaluation of the absorption coefficient explain the experimentally observed cutoff wavelengths and peak wavelength. However, they cannot explain why the responsivity spectrum is dominated by xy-polarized intersubband transitions. This can only be understood by considering the absorption spectrum and the vertical transport properties of the photoexcited carriers [13]. Holes excited to the HH2 state need a longer time to escape from the well, because they are still weakly bound. The lower escape probability and, hence, the lower gain, g leads to a lower responsivity [14]. In contrast, LH and SO states are higher in energy and have a smaller effective mass, so transport may be more efficient in these bands.

In conclusion we have investigated intersubband absorption and photoconductivity in pseudomorphic p-type SiGe/Si quantum wells in order to estimate their suitability for applications as sensitive quantum well infrared photodetectors (QWIP). The fabricated detector device shows a spectral response between 3 and 8 μm

† Note that absorption measurements on QWIP structures are often not conclusive due to the strong free-carrier absorption from the heavily doped contact layers. Instead, absorption measurements of similar structures without contact layers have been investigated in [7].

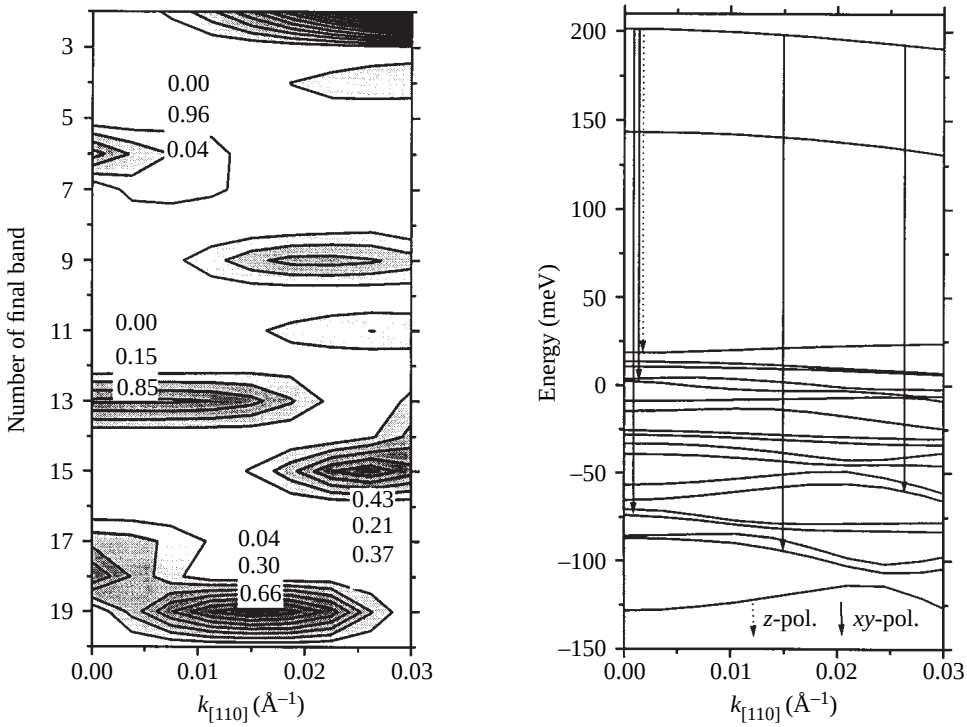

Fig. 4. Left panel: Contour plot of the oscillator strength for transitions from the HH ground state as a function of the final state's band number and the in-plane wavevector along the [110] direction for xy-polarized radiation. The triplet of numbers next to the regions of significant oscillator strength characterizes the contribution of HH, LH and SO valence bands to the final state. Right panel: In-plane dispersion along [110] for the first 20 eigenstates. Full arrows indicate xy-polarized transitions with high oscillator strength (identified in A). The broken arrow shows the HH1→HH2 transition which dominates the absorption of *z*-polarized light.

with a peak responsivity of $R_p = 76$ mA W^{-1} at $\lambda_p = 5$ μm under normal-incidence illumination. At the optimum bias point a detectivity $D^*_\lambda = 2 \times 10^{10}$ cm $\sqrt{\text{Hz}}$ W^{-1} is achieved. The desirable normal-incidence detection without the need for optical couplers is attributed to intersubband absorption of radiation polarized perpendicular to the growth direction which is possible due to the mixing of the HH, LH and SO valence bands.

References

[1] B. F. Levine, J. Appl. Phys. **74**, R1 (1993).

[2] S. D. Gunapala and K. M. S. Bandara, in *Homojunction and Quantum-Well Infrared Detectors*, eds M. H. Francombe and J. L. Vossen, Academic Press, San Diego: (1995).

[3] K. W. Goossen and S. A. Lyon, J. Appl. Phys. **63**, 5149 (1988); J. Y. Andersson and L. Lundqvist, Appl. Phys. Lett. **59**, 608 (1991).

[4] J. S. Park, R. P. G. Karunasiri, and K. L. Wang, Appl. Phys. Lett. **61**, 681 (1992); Appl. Phys. Lett. **61**, 2434 (1992); K. L. Wang and R. P. G. Karunasiri, in *Semiconductor Quantum Wells and Superlattices for Long-Wavelength Infrared Detectors*, edited by M. O. Manasreh, Artech, House, Boston: (1993).

[5] T. Fromherz, E. Koppensteiner, M. Helm, and G. Bauer, J. F. Nützel and G. Abstreiter, Phys. Rev. **B50**, 15073 (1994).

[6] R. People, J. C. Bean, C. G. Bethea, and L. J. Peticolas, Appl. Phys. Lett. **61**, 1122 (1992).

[7] T. Fromherz, P. Kruck, M. Helm, G. Bauer, J. F. Nützel, and G. Abstreiter, Appl. Phys. Lett. **68**, (1996).
[8] B. F. Levine, S. D. Gunapala, J. M. Kuo, S. S. Pei, and S. Hui, Appl. Phys. Lett. **59**, 1864 (1991).
[9] B.-Y. Tsaur, C. K. Chen, and S. A. Marino, IEEE Electron Device Lett. **12**, 293 (1991).
[10] J. S. Park, T. L. Lin, E. W. Jones, H. M. Del Castillo, and S. D. Gunapala, Appl. Phys. Lett. **64**, 2370 (1994).
[11] Y. C. Chang and R. B. James, Phys. Rev. **B39**, 12672 (1989).
[12] R. People and S. K. Sputz, Phys. Rev. **B41**, 8431 (1990).
[13] A. Fenigstein, E. Finkman, G. Bahir, and S. E. Schacham, J. Appl. Phys. **76**, 1998 (1994).
[14] H.C. Liu, Appl. Phys. Lett. **60**, 1507 (1992).